

## ARTICLE

# Dissociation Dynamics of Nitrous Oxide from Jet-cooling Absorption Spectrum in 142.5–147.5 nm

Cheng Zhen<sup>a</sup>, Ya-hua Hu<sup>b</sup>, Xiao-guo Zhou<sup>a\*</sup>, Shi-lin Liu<sup>a</sup>

*a.* Hefei National Laboratory for Physical Sciences at Microscale, Department of Chemical Physics, University of Science and Technology of China, Hefei 230026, China

*b.* College of Mathematics, Physics and Information Engineering, Jiaying University, Jiaying 314001, China

(Dated: Received on March 21, 2011; Accepted on April 6, 2011)

The absorption spectrum of the  $C^1\Pi$  state of  $N_2O$  molecule in the wavelength range of 142.5–147.5 nm has been measured under the jet-cooled condition, and the clear spectral features are displayed. A vibrational progression is observed with a frequency interval of about  $500\text{ cm}^{-1}$ . With the aid of potential energy surfaces (PES) of the low-lying electronic states of  $N_2O$ , the vibrational progression is assigned as the bending mode of the repulsive  $C^1\Pi$  state. From the Fourier transformation analysis, the recurrence period of the periodic orbit near the transition state region is derived to be 65 fs. Through the least-square Lorentzian fitting, the lifetimes of the resonance levels are estimated from their profile widths to be about 20 fs, which is shorter than the recurrence period. Therefore, a new explanation is suggested for the observed diffuse spectral structure, based on the behavior of dissociating  $N_2O$  on PES of the  $C^1\Pi$  state in the present excitation energy range.

**Key words:** Dissociation dynamic, Nitrous oxide, Jet-cooling, Absorption spectrum

## I. INTRODUCTION

Nitrous oxide ( $N_2O$ ) is one of the most important molecules in combustion and atmospheric chemistry [1], which has been proved to response partly to the greenhouse effect. In the atmosphere of earth, nitrous oxide can absorb ultraviolet radiation and then dissociate to produce the highly reactive oxygen atom in its first excited electronic state  $O(^1D)$ , which is recognized as a key role in the principal control mechanism limiting the  $O_3$  concentration in the stratospheric ozone layer. Moreover, the reaction of  $O(^1D)$  and  $N_2O$  is an important source of NO in the lower stratosphere [2].

The photo-absorption of nitrous oxide extends from 240 nm to the whole deep ultraviolet (UV) and vacuum UV (VUV) wavelength range. In the past several decades, photo-absorption processes of  $N_2O$  had attracted numerous experimental [3–37] and theoretical [38–45] investigations, and had been used as an important source of  $O(^1D)$  atoms in laboratory. The absorption coefficients in the 108–240 nm range had been measured [5–8, 17, 25], and the bands centered at 181, 146, and 129 nm had been assigned as transitions to the  $B^1\Delta$ ,  $C^1\Pi$ , and  $D^1\Sigma^+$  states, respectively [38]. Many experiments had been performed on the photodissociation dynamics of  $N_2O$  at wavelengths of 185 [7, 10],

193 [21], 203 [27, 28, 32, 37], 205 [19], and 207 nm [31]. The main dissociation fragments were  $N_2$  ( $X^1\Sigma_g^+$ ) and  $O(^1D)$  at these wavelengths, and the  $N_2$  fragment was highly rotationally excited and vibrational cold.

The second absorption band of  $N_2O$  was observed from 139 nm to 168 nm with the maximum at near 145 nm [4, 5, 17, 25]. The prominent spectral feature of this band showed a series of regular vibrational structures were superimposed over a continuous background, and it was assigned as the  $C^1\Pi \leftarrow X^1\Sigma^+$  electronic transition. Experimental investigations had been performed mainly on measurement of absorption cross section of the  $C^1\Pi$  state [5, 8, 9, 17, 25]. The dominant fragments were the O atoms and  $N_2$  molecules, while  $N(^2D)$  and NO fragments were almost neglectable [6, 11, 15, 17]. Based on the lack of knowledge about the PES of  $C^1\Pi$ , the earlier spectral assignments of the observed regular structures were illegible. Duncan assigned these regular diffuse bands as the bending excitation of  $N_2O$  [4], while Zelikoff *et al.* preferred the symmetric stretching vibration to the bending motion [5]. Recent measurement by Nee *et al.* evaded assigning the diffuse structure of the  $C^1\Pi$  state [25]. We know, with different vibrational modes excited on the upper electronic state, diverse dissociation mechanisms are probably expected. Therefore, a correct spectral assignment is serious to understand the dissociation dynamics of the  $C^1\Pi$  state, which is an important motivation for us to reinvestigate the absorption spectrum of  $N_2O$  molecule in the present excitation energy range.

\* Author to whom correspondence should be addressed. E-mail: xzhou@ustc.edu.cn

Besides experimental investigations, many theoretical works have been focused on dissociation of  $\text{N}_2\text{O}$  in the past decades [38–45], in which only a few [40, 44, 45] have explored the cut-through PESs of the electronically excited states. For the  $C^1\Pi$  state,  $\text{N}_2\text{O}$  is dissociative along the N–O bonding dimension both in collinear and bent geometry, but it is bound along the N–N coordinate at the Franck-Condon region. Recent theoretical investigations showed that the N–N–O angle changes in a large extent as  $\text{N}_2\text{O}$  is excited from the linear ground state to  $C^1\Pi$ , when the excitation energy is beyond the low barrier between the collinear and bent geometries [44, 45]. Therefore, the diffuse spectral structures of the  $C^1\Pi$  state do essentially reflect the dissociation behavior near the Franck-Condon region, not as the simple assignments by Duncan [4] and Zelikoff *et al.* [5]. The present work is aimed at the dissociation dynamic of  $C^1\Pi$ .

In order to elucidate the dissociate dynamics of  $\text{N}_2\text{O}$  molecules at the  $C^1\Pi$  state, a Fourier transformation is performed to translate the frequency-domain absorption spectrum to the time-domain autocorrelation function, which has been proved as a powerful tool to describe a periodic motion of wave packet on the excited PES [46]. As shown in examples of  $\text{CO}_2$  [47],  $\text{O}_3$  [48, 49], and  $\text{OCS}$  [50, 51], the recurrence peaks in the autocorrelation function indicate that, the diffuse structures over a broad continuous background in absorption spectrum correlate the vibrational motion of wave packet at the Franck-Condon region on the PES. The overall dissociation dynamics can be explained as a competition of wave packet motion between a fast dissociation along one dimension and a characteristic oscillation along another direction.

Since the Fourier transformation analysis can be contaminated by the vibrational and rotational congestion, it is necessary to reduce furthest these effects in an absorption spectrum. In the present study, we directly measure the absorption spectrum of  $\text{N}_2\text{O}$  in the 142.5–147.5 nm range, by utilizing a supersonic jet to reduce the intensities of vibrational hot bands and the widths of rotational contours. With the aid of the previous theoretical calculations, a clear description of the dissociation of  $\text{N}_2\text{O}$  on the PES of the  $C^1\Pi$  state is expected.

## II. EXPERIMENTS

The experimental setup includes a source of pulsed VUV laser generation, a pulsed supersonic molecule beam (MB), and two VUV intensity monitors. The time delay between the VUV laser and supersonic jet is controlled by a pulse generator (DG535, Stanford Research Systems). More details have been described elsewhere [52, 53]. Only a brief description is introduced here.

The third harmonic output from a pulsed Nd:YAG laser (Spectra-Physics, Lab-190-10, pulse width 10 ns) is split into two beams to pump simultaneously two

dye lasers (Sirah, PRLC-LG-18 and PRLC-LG-24). The VUV laser in 142.5–147.5 nm range is generated by two-photon resonance four-wave different frequency mixing in a krypton cell ( $\omega_{\text{VUV}}=2\omega_1-\omega_2$ ), where  $\omega_1$  corresponds to the frequency of two-photon excitation of krypton atom,  $(4p)^5(2P_{3/2})5p, [1/2]_0 \leftarrow (4p)^6, 1S_0$ , at  $2\omega_1=94093.66 \text{ cm}^{-1}$ . Tunability of the VUV laser is produced by scanning the wavelength of the other dye laser  $\omega_2$ . The generated VUV laser from the Kr cell is separated from the two fundamentals,  $\omega_1$  and  $\omega_2$ , by a LiF prism in a vacuum chamber. Finally, only the collinear VUV laser is led into the absorption chamber. The VUV laser crosses with the jet-cooled pure  $\text{N}_2\text{O}$  (stagnation pressure 121.2 kPa, mixing with less than 1%CO) beam at 5 mm downstream from the nozzle orifice.

For the direct measurements of absorption spectrum under jet-cooling conditions, two LiF plates are inserted in the propagation pathway of VUV laser beam at positions prior to and after absorption by the jet-cooled molecular beam (MB), to monitor the relative VUV intensities with two photomultiplier tubes (Electron Tubes, 9403B). A VUV absorption spectrum is recorded finally from transformation of the Beer-Lambert law,

$$I_l(\lambda) = I_0(\lambda)e^{-N\sigma(\lambda)l} \quad (1)$$

where  $I_0(\lambda)$  and  $I_l(\lambda)$  represent respectively the VUV intensities prior to and after the absorption,  $N$ ,  $\sigma(\lambda)$ , and  $l$  are molecular number density, absorption cross section at wavelength  $\lambda$ , and absorption path length, respectively. Since the sensitivities of the two photomultiplier tubes are slight different although they are of the same type, two individual measurements have to be performed, *i.e.*, with the pulse MB valve on and off. Consequently, the absorption cross section  $\sigma(\lambda)$  can be expressed as,

$$\sigma(\lambda) \propto \ln \frac{I_l(\lambda)/I_0(\lambda)}{I'_l(\lambda)/I'_0(\lambda)} \quad (2)$$

where  $I'_0(\lambda)$  and  $I'_l(\lambda)$  are the VUV intensities prior to and after the absorption, when the supersonic jet is turned off. In this way, the shot-to-shot fluctuation of VUV intensity, the variation of VUV intensity with wavelength, as well as the sensitivity difference of photomultiplier tubes, can be normalized, and hence the detection limit of absorption spectrum can be increased greatly. Our recent measurement on the absorption spectrum of jet-cooled  $\text{OCS}$  molecule showed, that less than 1% of the VUV intensity reduction by absorption can be definitely detected, although the shot-to-shot intensity fluctuation of the VUV laser generated by four-wave frequency mixing is more than 40% [53].

In order to increase the VUV absorption path length, a commercial slit nozzle (General valve, 0.12 mm×12 mm) is used to produce a slit MB along the propagation direction of VUV laser. The wavelength and linewidth of VUV laser are calibrated with

TABLE I Peak positions  $\nu$ , widths  $\Gamma$ , and estimated lifetimes  $\tau$ , for the distinct features in the absorption spectrum of the  $C^1\Pi\leftarrow X^1\Sigma^+$  transition of jet-cooled  $N_2O$ , and the corresponding results of the Fano-profile analysis for this spectrum, including the asymmetric parameter  $q$ .

Peak	Assign.	Lorentzian profile analysis <sup>a</sup>			Fano profile analysis <sup>c</sup>		
		$\nu^b/cm^{-1}$	$\Gamma/cm^{-1}$	$\tau/fs$	$\nu/cm^{-1}$	$\Gamma/cm^{-1}$	$q$
a	$\nu_{TS}$	67793 (67897)	(237)				
b	$\nu_{TS}+1$	68314±12 (68369)	186±2 (320)	28	68330±13	123±4	-2.3±0.1
c	$\nu_{TS}+2$	68828±22 (68841)	282±3 (380)	19	68834±24	176±3	-12.2±0.8
d	$\nu_{TS}+3$	69305±30 (69318)	240±3 (469)	22	69313±47	163±7	-25.7±9.0
e	$\nu_{TS}+4$	69770±45 (69792)	312±10 (380)	17			
f	$\nu_{TS}+5$	70220 (70263)	(504)				

<sup>a</sup>  $\nu$  and  $\Gamma$  in parentheses are derived from the least-square Lorentzian fit of the plotted spectrum of reading points shown as the solid line in Fig.1.

<sup>b</sup> For the a and f peaks, peak positions were estimated, because only a half peak profiles of them were recorded in the present jet-cooled absorption spectrum.

<sup>c</sup> The absorption intensity of the e peak is too weak to be effectively fitted with a Fano-profile.

the laser-induced fluorescence (LIF) spectrum of CO ( $A^1\Pi\leftarrow X^1\Sigma^+$ ) at about 142 nm. The linewidth of VUV laser is estimated to be about  $0.3\text{ cm}^{-1}$  from the linewidth of individual rotational transition in the CO LIF spectrum, and a rotational temperature of about 40 K is derived from its spectral simulation. Under the same expansion conditions, the rotational temperature of  $N_2O$  is expected to be around 40 K. It should be emphasized that the contributions of absorption of CO ( $A^1\Pi\leftarrow X^1\Sigma^+$ ) are neglectable for the present absorption spectrum of  $N_2O$  in 142.5–147.5 nm because of its much lower intensity. Commercial gas samples of  $N_2O$  and CO (>99.8%, GC grade) have been used without any further purification.

### III. RESULTS AND DISCUSSION

#### A. Overall features of the absorption spectrum

Figure 1 shows the absorption spectrum of  $N_2O$  in excitation energy range of  $67750\text{--}70250\text{ cm}^{-1}$ . Our data measured under jet-cooled condition is plotted as the dots in Fig.1, and the previous absorption spectrum recorded at room temperature in a flowing cell by Nee *et al.* is shown as the solid line for comparison, which was obtained by reading points of the enlarged copy of the published spectrum [25]. Briefly, six major resonance peaks (a–f in Fig.1) are involved in both spectra with a spectral interval of about  $500\text{ cm}^{-1}$ , and only the half profiles of the lowest and the highest peaks are recorded in this study, due to the wavelength limitation of scanning range of  $\omega_2$  dye laser.

Obviously, the widths of resonance peaks become generally narrower in the present measurement than that at room temperature. By fitting both spectra with Lorentzian profiles, the widths and the positions of resonance peaks are obtained and summarized in Table I. Figure 2 shows the fitting profile of the present spec-

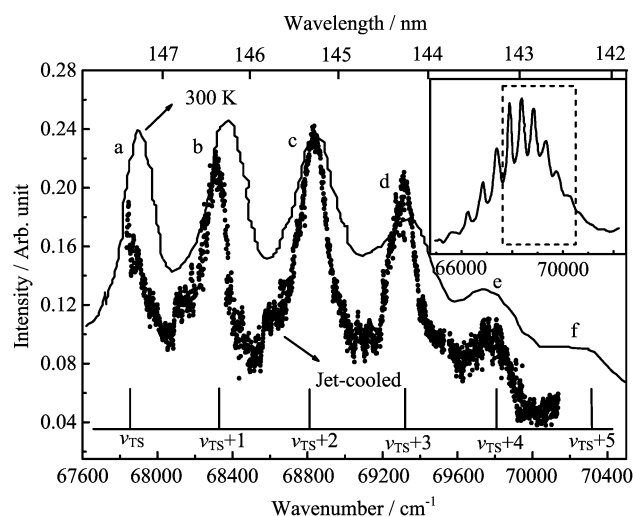


FIG. 1 The absorption spectra of  $N_2O$ , measured under jet-cooled conditions in present work (dotted line) and at room temperature in a flowing cell (solid line) by Nee *et al.* [25]. The entire absorption spectrum of the  $C^1\Pi\leftarrow X^1\Sigma^+$  electronic transition at room temperature in Ref.[25], where the dashed line pane notes the present excitation energy range.

trum, where six peaks were used in the spectral fitting with the Lorentzian profiles to obtain a satisfactory reproduction of the overall experimental spectrum. In the fitting process, the resonance wavelength  $\lambda$  and width  $\Gamma$  of the a and f peaks in Fig.1 were estimated and kept. Generally, there are three possible effects to broaden a vibrational band, *i.e.*, homogeneous broadening due to a fast dissociation in the Franck-Condon region, broadening of band contours by vibrationally and rotationally hot populations at the ground state, and the spectral resolution determined by the light source. Since the previous absorption spectra were measured with the light

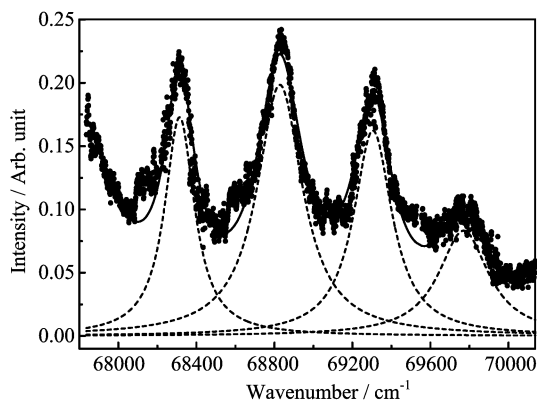


FIG. 2 Experimental (dotted) and fitted (dashed line) absorption spectra of  $\text{N}_2\text{O}$  in 142.5–147.5 nm, where the dashed lines show the Lorentzian profiles of individual vibrational resonances.

from a monochromator and at room temperatures [5, 25], the spectral resolution was about  $50\text{ cm}^{-1}$  in the VUV range, whilst the spectral broadening by vibrationally and rotationally hot population would be expected. Therefore, the true spectral width caused by dissociation could not be measured exactly from the previous experiments. On the contrary, the spectral resolution in this absorption spectrometer is estimated to be  $0.3\text{ cm}^{-1}$  from the individual rotational linewidth in the CO LIF spectrum, and more significantly, sufficient vibrational and rotational cooling (40 K) is obtained. Therefore, the widths and profiles in present absorption spectrum directly reflect the dissociation dynamics on the electronically excited PES.

It is clearly seen from Fig.1, that the widths of resonance peaks decreased dramatically from near  $400\text{ cm}^{-1}$  at room temperature to about  $250\text{ cm}^{-1}$  under jet-cooled conditions, implying that the influences of the low spectral resolution and vibrational/rotational hot populations are serious in the previous absorption spectra. In addition, the widths of the b, c, d, and e peaks in Fig.1(a) show an increasing trend consistently with the excitation energy. Interestingly, the spectral profiles of all prominent peaks in the jet-cooling absorption spectrum show more or less asymmetric, which is potentially caused by the dissociating behavior of  $\text{N}_2\text{O}$  on PES.

### B. Spectral assignments of the absorption spectrum

Although Hopper suggested that the  $d^3\Pi \leftarrow X^1\Sigma^+$  transition could extend to the present excitation energy range, its intensity would be very limited due to the spin-forbidden [40]. Previous theoretical [38, 40, 44, 45] and experimental [15, 25] studies have obtained an agreement that the overall absorption spectrum in the excitation energy range between  $64500$  and  $72000\text{ cm}^{-1}$  mainly corresponds to the  $C^1\Pi \leftarrow X^1\Sigma^+$  transition of  $\text{N}_2\text{O}$ . However, the observed vibrational progression has

not been definitely assigned. Zelikoff *et al.* obtained a vibrational frequency of  $1005\text{ cm}^{-1}$  by a polynomial fitting and an abnormal strong anharmonicity [5]. Thus the vibrational progression had been assigned as excitation of the symmetric stretching vibration of  $\text{N}_2\text{O}$ , just because the frequency was the most close to the symmetric stretching frequency,  $1285\text{ cm}^{-1}$ , among all three vibrational frequencies of the ground electronic state [54]. Apparently, this assignment strongly depended on the order of the used polynomial, and the abnormal anharmonicity was unreasonable. In addition, the vibrational and rotational hot populations were overlapped seriously in the previous absorption spectra, as the experiments had been done at room temperature in flowing cell. Thus, the previous spectral assignment should be doubted. More significantly, the dissociating characteristics of the  $C^1\Pi$  state were not considered. As the theoretical calculations suggested [44, 45] the  $C^1\Pi$  state is fast dissociative along the N–O stretch coordinate, thus  $\text{N}_2\text{O}(C^1\Pi)$  is expected to dissociate in femto-second timescale. Therefore the distinct vibrational progression could not be assigned to any classical normal vibrational mode as Zelikoff *et al.* did [5].

Generally, a diffuse spectral structure for a dissociating state can reflect its vibrational motion orthogonal to the reaction coordinate in the transition state region. A typical example is the  $D^1B_2 \leftarrow X^1A_1$  transition of  $\text{O}_3$  molecule in excitation energy range of  $28600$ – $42269\text{ cm}^{-1}$ , where the weak diffuse resonance peaks are observed over the broad absorption band, and the vibrational structures are assigned to particular types of unstable periodic or nearly periodic orbits in the classical dynamics [48, 49]. Our present case is very similar to that of  $\text{O}_3$  molecule. Once the  $\text{N}_2\text{O}$  is excited to the  $C^1\Pi$  state, the fast dissociation along N–O coordinate is expected, whilst a large-amplitude bending motion is strongly active as well. Therefore, although there is no wave packet calculation performed on the PES of  $C^1\Pi$  state, the observed vibrational progression is indeed referred to the excitation of the transition-state vibrational mode, which can be correlated to an unstable periodic or nearly periodic orbit on the PES of  $C^1\Pi$ . Since the progression spacing of about  $500\text{ cm}^{-1}$  is really close to the bending vibrational frequency,  $589\text{ cm}^{-1}$ , of the ground state, the observed six peaks are expected to correlate to the bending motion of transition state.

As we know, an electronic absorption spectrum, *i.e.* the absorption cross section  $\sigma(E)$  generally as a function of an excitation energy  $E$ , is always correlated to the dynamics of the wave packet motion on PES. Their relationship can be presented by the Fourier transformation in the following formula [55, 56],

$$\sigma(E) \propto \int_{-\infty}^{+\infty} e^{iEt/\hbar} \langle \Phi(t) | \Phi(0) \rangle dt \quad (3)$$

where  $\Phi(0)$  is the initial wave packet placed on the Franck-Condon region on the PES, and  $\Phi(t)$  is the wave

packet at time of  $t$ . Thus,  $\langle \Phi(t) | \Phi(0) \rangle$  is the dipole-dipole autocorrelation function, and hence its quantity can be obtained by an inverse Fourier transformation integral over the absorption cross section. In this way, the dissociation dynamics on the excited PES of various molecules, such as  $\text{CO}_2$  [47],  $\text{O}_3$  [48, 49], and  $\text{OCS}$  [50, 51] have been discussed.

After eliminating the influences of vibrational hot bands and rotational broadening due to jet-cooling, a Fourier transformation analysis of the absorption spectrum can directly provide dynamic information of the  $C^1\Pi$  state, which is shown in Fig.3. A clear prominent recurrence is identified at  $t=65$  fs in the autocorrelation function. In a simple paradigm of propagating a coherent Gaussian wave packet, recurrences indicate a return or near return of the whole packet to its original configuration [57, 58]. Therefore, the recurrence in Fig.3 implies that the wave packet placed in the Franck-Condon region on PES of the  $C^1\Pi$  state is trapped for a while in the vicinity of an unstable periodic or nearly periodic orbit, which is perpendicular to the dissociation coordinate. The period of 65 fs in Fig.3 corresponds to a vibrational frequency  $513\text{ cm}^{-1}$ , which is actually very close to the observed progression interval (about  $500\text{ cm}^{-1}$ ) of the six resonances. Moreover, the close values of the frequency,  $513\text{ cm}^{-1}$ , and the bending frequency ( $589\text{ cm}^{-1}$ ) of the ground state, support us to attribute the vibrational motion of transition state to the bending mode. In addition, the previous Fourier transformation analysis of the overall absorption spectrum in excitation energy range of  $64500\text{--}72000\text{ cm}^{-1}$  also suggested a recurrence period of 66 fs [59], indicating that only the bending mode of the  $C^1\Pi$  state contributes the unstable periodic or nearly periodic orbit.

Generally, an accurate lifetime can not be defined from the FWHM when the profile of the absorption peak is asymmetrical, because the decay process is not simply described with a single exponential. However as an approximate estimation, the lifetimes of these resonance levels were derived from their homogeneous bandwidths and list in Table I as well. Since the profiles of the a and f peaks were not measured fully in the present experiment, and thus their FWHMs and lifetimes could be arbitrary in a certain extent in the fitting process. Thus we do not involve their results in Table I.

Obviously with the excitation energy increasing, the lifetimes of these resonance levels have a slightly decreasing trend, all of which are near 20 fs and shorter than one oscillation period of the unstable periodic (or nearly periodic) orbit, 65 fs. It indicates that  $\text{N}_2\text{O}$  molecule dissociate instantaneously in the present excitation energy range, prior to oscillate and return to its starting position. In this case, no vibrational progression derived from the unstable periodic orbit could be expected. Therefore, the progression can not be assigned to an unstable periodic orbit at the transition state region, and needs to be explained in a different

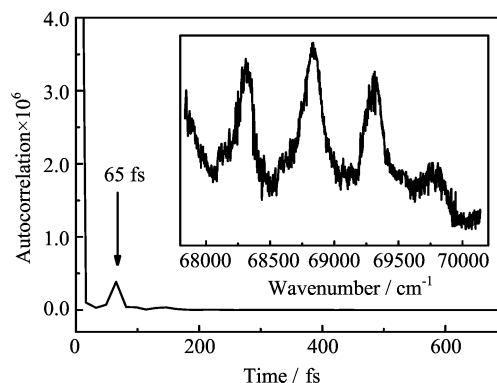


FIG. 3 Autocorrelation function obtained from the Fourier transform of the absorption spectrum of the  $C^1\Pi \leftarrow X^1\Sigma^+$  transition of jet-cooled  $\text{N}_2\text{O}$ . The present absorption spectrum is shown in the insert panel as well.

way. The best candidate is that a stable periodic orbit from the bending mode of the  $C^1\Pi$  state causes this vibrational progression. We will discuss the dissociation dynamics in the following sections.

### C. Asymmetric peak profile analysis

As shown in Fig.1, the profiles of the present vibrational bands present more or less asymmetry. Based on the fact that the observed vibrational progression refers to the excitation of the transition-state vibrational mode, the Fano-type profile [60], as a typical asymmetric profile, is expected for the resonance levels in the  $C^1\Pi$  state, which is potentially caused by a quantum coupling between a quasi-bound state and a zero-order continuum state. In a Fano-type asymmetric profile system, the absorption spectrum  $I(E)$  can be expressed in terms of  $q$  [60],

$$I(E) = \sigma_b + \sigma_0 \frac{(q + \varepsilon)^2}{1 + \varepsilon^2} \quad (4)$$

$$\varepsilon = \frac{E - E_\Gamma}{\Gamma/2} \quad (5)$$

where  $E_\Gamma$  and  $\Gamma$  present respectively the position of resonance peak and its width,  $\sigma_b$  and  $\sigma_0$  are the absorption cross sections to the continua, which are irrelevant and relevant to the interference, respectively.  $q$  reflects the interference between the quasi-bound and dissociative states, and it can be positive or negative values, which will lead the peak profile shade toward the higher and lower energy sides, respectively. The smaller is the absolute value of  $q$ , the larger the asymmetric degree of spectral profile is.

The absorption spectrum was fitted by the least-square Fano-type profiles, and shown in Fig.4.  $\Gamma$  and  $q$  are summarized in Table I as well. The positions of resonance peaks are consistent in both fitted results with Lorentzian and Fano-type profiles. For the b, c, and

d peaks in Fig.4, the FWHM widths from Fano-profile fitting are much narrower than those from Lorentzian fitting, *e.g.* the width of the c peak is  $282\text{ cm}^{-1}$  from Lorentzian profile fitting, and decreases to  $176\text{ cm}^{-1}$  from Fano-type profile fitting. Therefore the lifetimes of the resonance levels should be slightly longer than the values in Table I estimated from Lorentzian profile analysis, however they are still shorter than one aforementioned oscillation period, 65 fs.

As shown in Table I, the  $q$  decreases gradually from  $-2.3$  (b peak) to  $-25.7$  (d peak) in Fig.4, and shows an apparent dependence on the vibrational quantum number. Additionally, it is not similar to the case of another similar linear molecule, OCS. For the excited  ${}^1\Sigma^+$  state of OCS, a  $q$ -reversal phenomenon was found in its absorption spectrum [50, 51]. As the  $\nu_{\text{TS}}$  increasing, the  $q$  decreased firstly from a small negative value, then reversed quickly backwards to a positive value. Thus the different  $\nu_{\text{TS}}$  dependent behaviors of  $q$  in the absorption spectra of  $\text{N}_2\text{O}$  and OCS molecule imply the different features of PES of the excited electronic state. The multichannel quantum defect theory (MQDT) shows that [61], this  $q$ -reversal phenomenon is caused by an interference from the third interloper state in addition to the two interacting discrete and continuum states. Two probable explanations were suggested for the  $q$ -reversal observed in OCS molecule [51]: a small hump exists on the PES along the dissociation coordinate near the Franck-Condon region, or alternatively, a substantial change of the nodal pattern of the zero-order vibrational wavefunction of the transition state results in a change of the overlap integral between it and the electronic ground state. Therefore, both the special characteristics mentioned above do not exist in the case of the  $C^1\Pi$  state of  $\text{N}_2\text{O}$ .

#### D. Transition state dynamics in the $C^1\Pi$ excited state

In order to understand properly dissociation dynamics of the  $C^1\Pi$  state, its all-dimension PES and wave packet calculations are necessary. Unfortunately, there is none PES of this type published up to now. Only a few theoretical investigations [40, 44, 45] were performed to describe cut through potential energy curves of the  $C^1\Pi$  state along the N–O, N–N bonding, and bending coordinates, respectively.

Based on the estimated lifetimes of vibrational bands in Table I and the recurrence period obtained from the Fourier transformation analysis, a rough image of dissociating  $\text{N}_2\text{O}$  on PES of the  $C^1\Pi$  state in the present excitation energy range can be predicted: the wave packet in the Franck-Condon region of the  $C^1\Pi$  state is a superposition of the dissociative wave functions that have many nodes along the bending motion, and therefore, it immediately dissociates due to the steep repulsive slope of the  $C^1\Pi$  state along the N–O coordinate, while the bending excited vibrational levels are blurred by the uncertainty principle. In other words, the observed vi-

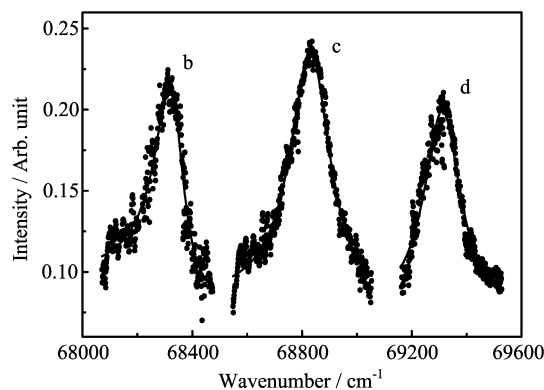


FIG. 4 Experimental (circle) and fitted (solid line) absorption spectra of  $\text{N}_2\text{O}$  ( $C^1\Pi$ ), where the Fano-type profiles of individual resonance bands are used in spectral fitting.

brational progression correlates to the bending motion of the  $C^1\Pi$  state indeed, however the levels are seriously broadened due to fast dissociation along the N–O coordinate.

It needs to be emphasized that the bending and the dissociating N–O stretching degree of freedom probably are not adiabatically separated in the present energy range, as they do in potential well like the bound states. The classical vibrational motion probably behaves chaotically, and a coupling exists between them. Thus, simple one-dimensional bending wavefunctions do not exist in this case. That is to say, although a set of quantum numbers,  $\nu_{\text{TS}}$ , is used here to label the spectral structures of this  $C^1\Pi$  state, they do not present actually the classical normal bending motions. As mentioned above, the energy intervals between all “vibrational bands” in the spectrum only present approximately the “bending” vibrational frequencies.

#### IV. CONCLUSION

The absorption spectrum of the  $C^1\Pi$  state of nitrous oxide in the wavelength region of 142.5–147.5 nm was measured under the jet-cooled condition. A vibrational progression was observed with a frequency interval of about  $500\text{ cm}^{-1}$ . Due to sufficient vibrational and rotational cooling of  $\text{N}_2\text{O}$ , the clearer spectral features were displayed than the previous ones measured at room temperature in a flowing cell, *e.g.* the narrower vibrational band widths. The widths of these resonance peaks were derived from a least-square Lorentzian profile fitting, and hence the corresponding lifetimes were estimated subsequently to be about 20 fs. Moreover, the progression spacing of about  $500\text{ cm}^{-1}$  is close to the bending frequency ( $589\text{ cm}^{-1}$ ) of the ground electronic state. Therefore, with the aid of PES of the low-lying electronic state of  $\text{N}_2\text{O}$ , the vibrational progression was assigned as the bending resonances of the  $C^1\Pi$  state.

The Fourier transformation analysis of the absorption

spectrum indicated a 65 fs recurrence time of an unstable periodic (or nearly periodic) orbit near the transition state, which corresponds to a frequency interval of  $513\text{ cm}^{-1}$  and is close to the observed progression interval (about  $500\text{ cm}^{-1}$ ). Compared with the oscillation period of 65 fs, the lifetimes of the resonances are much shorter. Therefore, the unstable periodic orbit can not explain the spectral diffuse structure, and a new explanation is suggested: the wave packet in the Franck-Condon region of the  $C^1\Pi$  state is a superposition of the dissociative wave functions that have many nodes along the bending motion, and thus it immediately dissociates due to the steep repulsive slope of the  $C^1\Pi$  state along the N–O coordinate, whilst the bending excited vibrational levels are blurred by the uncertainty principle.

Besides spectral and dissociation dynamical conclusions, the asymmetric line profiles were observed in the absorption spectrum. Based on the theoretical investigations, the Fano-type asymmetric profiles were used in the least-square multi-peak fitting of absorption spectrum. The corresponding asymmetric parameters  $q$  were derived and presented the dependence on the  $\nu_{\text{TS}}$  quantum number. However it was distinct with the  $q$ -reversal phenomenon of another similar linear molecule, OCS, indicating that the wavefunctions on the excited electronic state of  $\text{N}_2\text{O}$  and OCS have different physical characteristics.

## V. ACKNOWLEDGMENTS

This work was supported by the National Natural Science Foundation of China (No.10979042 and No.21073173), the National Key Basic Research Special Foundation of China (No.2007CB815204), and the Fundamental Research Funds for the Central Universities. Authors also would like to thank Prof. J. B. Nee to provide his experimental data for our reference.

[1] R. P. Wayne, *Chemistry of Atmospheres*, 3rd Edn., Oxford: Oxford University Press, (2000).  
 [2] M. Nicholet and W. Peetermans, *Ann. Geophys.* **28**, 751 (1972).  
 [3] S. W. Leifson, *Astrophys. J.* **63**, 73 (1926).  
 [4] A. B. F. Duncan, *J. Chem. Phys.* **4**, 638 (1936).  
 [5] M. Zelikoff, K. Watanabe, and E. C. Y. Inn, *J. Chem. Phys.* **21**, 1643 (1953).  
 [6] M. Zelikoff and L. M. Aschenbrand, *J. Chem. Phys.* **22**, 1680 (1954).  
 [7] M. Zelikoff and L. M. Aschenbrand, *J. Chem. Phys.* **22**, 1685 (1954).  
 [8] B. A. Thompson, P. Harteck, and P. R. Reeves Jr., *J. Geophys. Res.* **68**, 6431 (1963).  
 [9] J. Y. Yang and F. M. Servedio, *J. Chem. Phys.* **47**, 4817 (1967).  
 [10] N. R. Greiner, *J. Chem. Phys.* **47**, 4373 (1967).

[11] R. G. Young, G. Black, and T. G. Slanger, *J. Chem. Phys.* **49**, 4769 (1968).  
 [12] J. W. Rabalais, J. M. McDonald, V. Scherr, and S. P. McGlynn, *Chem. Rev.* **71**, 73 (1971).  
 [13] K. F. Preston and R. F. Barr, *J. Chem. Phys.* **54**, 3347 (1971).  
 [14] H. S. Johnston and G. S. Selwyn, *Geophys. Res. Lett.* **2**, 549 (1975).  
 [15] G. Black, R. L. Sharpless, T. G. Slanger, and D. C. Lorents, *J. Chem. Phys.* **62**, 4266 (1975).  
 [16] G. S. Selwyn and H. S. Johnston, *J. Chem. Phys.* **74**, 3791 (1981).  
 [17] L. C. Lee and M. Suto, *J. Chem. Phys.* **80**, 4718 (1984).  
 [18] P. Felder, B. M. Haas, and J. R. Huber, *Chem. Phys. Lett.* **186**, 177 (1991).  
 [19] N. Shafer, K. Tonokura, Y. Matsumi, S. Tasaki, and M. Kawasaki, *J. Chem. Phys.* **95**, 6218 (1991).  
 [20] T. F. Hanisco and A. C. Kummel, *J. Phys. Chem.* **97**, 7242 (1993).  
 [21] L. L. Springsteen, S. Satyapal, Y. Matsumi, L. M. Dobeck, and P. L. Houston, *J. Phys. Chem.* **97**, 7239 (1993).  
 [22] W. F. Chan, G. Cooper, and C. E. Brion, *Chem. Phys.* **180**, 77 (1994).  
 [23] T. Suzuki, H. Katayanagi, Y. Mo, and K. Tonokura, *Chem. Phys. Lett.* **256**, 90 (1996).  
 [24] J. B. Nee, J. C. Yang, P. C. Lee, X. Y. Wang, and C. T. Kuo, *J. Phys. B* **31**, 5175 (1998).  
 [25] J. B. Nee, J. C. Yang, P. C. Lee, X. Y. Wang, and C. T. Kuo, *Chin. J. Phys.* **37**, 172 (1999).  
 [26] M. Ahmed, E. R. Wouters, D. S. Peterka, O. S. Vasutinskii, and A. G. Suits, *Faraday Discuss.* **113**, 425 (1999).  
 [27] D. W. Neyer, A. J. R. Heck, and D. W. Chandler, *J. Chem. Phys.* **110**, 3411 (1999).  
 [28] D. W. Neyer, A. J. R. Heck, D. W. Chandler, J. M. Teule, and M. H. M. Janssen, *J. Phys. Chem. A* **103**, 10388 (1999).  
 [29] J. M. Teule, G. C. Groenenboom, D. W. Neyer, D. W. Chandler, and M. H. M. Janssen, *Chem. Phys. Lett.* **320**, 177 (2000).  
 [30] M. Brouard, P. O'Keeffe, M. D. Joseph, and D. Minayev, *Phys. Rev. Lett.* **86**, 2249 (2001).  
 [31] S. F. Adams, C. A. DeJoseph Jr., C. C. Carter, T. A. Miller, and J. M. Williamson, *J. Phys. Chem. A* **105**, 5977 (2001).  
 [32] A. M. Rijs, E. H. Backus, C. A. de Lange, M. H. M. Janssen, K. Wang, and V. McKoy, *J. Chem. Phys.* **114**, 9413 (2001).  
 [33] C. Cossart-Magos, M. Jungen, and F. Launay, *J. Chem. Phys.* **114**, 7368 (2001).  
 [34] B. R. Cosofret, H. M. Lambert, and P. L. Houston, *Bull. Korean Chem. Soc.* **23**, 179 (2002).  
 [35] E. Bustos, A. M. Velasco, I. Martin, and C. Lavin, *J. Phys. Chem. A* **106**, 35 (2002).  
 [36] M. Brouard, A. P. Clark, C. Vallance, and O. S. Vasutinskii, *J. Chem. Phys.* **119**, 771 (2003).  
 [37] H. Kawamata, H. Kohguchi, T. Nishide, and T. Suzuki, *J. Chem. Phys.* **125**, 133312 (2006).  
 [38] N. W. Winter, *Chem. Phys. Lett.* **33**, 300 (1975).  
 [39] C. Frind, L. Asbrink, and F. Lindholm, *Chem. Phys.* **27**, 169 (1978).  
 [40] D. G. Hopper, *J. Chem. Phys.* **80**, 4290 (1984).

- [41] A. T. Wong and G. B. Bacskay, *Chem. Phys. Lett.* **207**, 360 (1993).
- [42] A. Brown, P. Jimeno, and G. Balint-Kurti, *J. Phys. Chem. A* **103**, 11089 (1999).
- [43] M. S. Johnson, G. D. Billing, A. Gruodis, and M. H. M. Janssen, *J. Phys. Chem. A* **105**, 8672 (2001).
- [44] S. Nanbu and M. S. Johnson, *J. Phys. Chem. A* **108**, 8905 (2004).
- [45] M. N. Daud, G. G. Balint-Kurti, and A. Brown, *J. Chem. Phys.* **122**, 054305 (2005).
- [46] R. Schinke, *Photodissociation Dynamics*, Cambridge: Cambridge University Press, (1993).
- [47] R. Schinke and V. Engel, *J. Chem. Phys.* **93**, 3252 (1990).
- [48] B. R. Johnson and J. L. Kinsey, *Phys. Rev. Lett.* **62**, 1607 (1989).
- [49] B. R. Johnson and J. L. Kinsey, *J. Chem. Phys.* **91**, 7638 (1989).
- [50] K. Yamanouchi, K. Ohde, A. Hishikawa, and C. D. Pibel, *Bull. Chem. Soc. Jpn.* **68**, 2459 (1995).
- [51] A. Hishikawa, K. Ohde, R. Itakura, S. Liu, K. Yamanouchi, and K. Yamashita, *J. Phys. Chem. A* **101**, 694 (1997).
- [52] Q. F. Li, H. Wang, Y. Shi, J. H. Dai, S. L. Liu, S. Q. Yu, and X. X. Ma, *Chin. J. Chem. Phys.* **17**, 333 (2004).
- [53] Q. F. Li, H. Wang, Y. Q. Yu, S. L. Liu, S. Q. Yu, and X. X. Ma, *Chin. J. Chem. Phys.* **18**, 474 (2005).
- [54] G. Herzberg, *Molecular Spectra and Molecular Structure III, Electronic Spectra of Polyatomic Molecules*, New York: Van Nostrand, (1966).
- [55] E. J. Heller, *J. Chem. Phys.* **68**, 2066 (1978).
- [56] K. C. Kulander and E. J. Heller, *J. Chem. Phys.* **69**, 2439 (1978).
- [57] E. J. Heller, *Acc. Chem. Res.* **14**, 368 (1981).
- [58] E. J. Heller, R. Sundberg, and D. Tannor, *J. Phys. Chem.* **86**, 1822 (1982).
- [59] C. Zhen, Y. H. Hu, S. L. Liu, and X. G. Zhou, *Acta Phys. Chim. Sin.* **26**, 94 (2010).
- [60] U. Fano, *Phys. Rev.* **124**, 1866 (1961).
- [61] A. Giusti-Suzor and H. Lefebvre-Brion, *Phys. Rev. A* **30**, 3057 (1984).